Full Length Research Paper

Numerical calculation of the electron mobility in ZnS and ZnSe semiconductors using the iterative method

M. Rezaee Rokn-Abadi

Physics Department, Ferdowsi University of Mashhad, Mashhad, Iran. E-mail: roknabad@um.ac.ir.

The electron mobility of ZnS and ZnSe semiconductor compounds were calculated by using the iteration method. We considered polar optical phonon scattering, deformation potential acoustic, piezoelectric and ionized impurity scattering mechanisms. Band nonparabolicity, admixture of p functions, arbitrary degeneracy of the electron distribution, and the screening effects of free carriers on the scattering probabilities are incorporated. We investigated temperature and doping dependencies of mobility for the given compounds. The electron mobility of the two materials was found to be similar, though the ZnS characteristics were on the whole superior. It is also found that the electron mobility decreases monotonically as the temperature increases from 100 to 600 K for two crystal structures. The low temperature value of electron mobility increases significantly with increasing doping concentration.

Key words: Electron mobility, piezoelectric, ionized impurity, nonparabolicity.

INTRODUCTION

The transport properties of ZnS and ZnSe have been a subject of extensive investigation in recent years (Chen et al., 1998). There has been a great interest in the study of charge carrier transport of ZnS and ZnSe due to the wide band gap, which has become one of the most applied insulators in thin-film electro luminescence devices (Look et al., 1998). Most previous studies have assumed the electron distribution function of cool temperature with high-energy tail ends at less than 4 eV. Makino et al. (2001) have used a single parabolic band in the first conduction band. This is at very high field unrealistic. The full band details of the first two conduction bands as well as full-order treatment of the electron phonon interaction have been included by Brennan (1998). Electron transport at low electric field was calculated for the first time by solving the Boltzmann transport equation, exactly under generalized Fermi-Dirac statistics for the most scattering events. Electron mobility and resistivity were calculated as a function of electron concentration at both 300 and 77 K (Di and Brennan, 1991). Mansour et al. (2000) used a model that included only the first conduction in a nonparabolic three valleys model. Chattopadhyay and Queisser (1981) have developed a model including a nonparabolic three valleys of the first conduction band and a single valley in the second conduction band. Using the pseudopotential

method, the density of states in the last case was included. Most of the pervious theoretical work on transport properties of ZnS and ZnSe, in high electric field, and at room temperature has been mainly based on Monte Carlo method. The temperature and doping dependencies of electron mobility in ZnS and ZnSe are of particular relevance to the large effort at present to producing AC and DC electro luminscent devices. AC electro luminscent devices were made by encapsulating large band gap semiconductors such as ZnS: Mn or ZnSe: Mn by two insulates layers, typically Y_2O_3, on either side of the semiconductor layers. An AC bias applied across the device alternately accelerates the electrons from one semiconductor insulator interface to the other. An electro luminscent phenomenon occurs when the free carriers are accelerated to sufficiently high energy, such that impact excitation of the Mn center becomes possible.

In ZnS and ZnSe semiconductor compounds the dominant scattering mechanisms is primarily the polar optic phonon scattering mechanism. The others are ionized impurity scattering, acoustic phonon deformation potential scattering and acoustic phonon piezoelectric scattering mechanisms (Moglestue, 1993). As a result of being elastic process of acoustic phonon deformation potential scattering, acoustic piezoelectric scattering and

ionized impurity scattering, their mobilities can be calculated with the relaxation time approach. But if the electron energy can be compared with the phonon energy, this is important and such a scattering is inelastic scattering. The compensated changing in the energy is taken place after inelastic scattering. Since in inelastic scattering process the phonon energy is the bigger than the electron energy. Thus, relaxation time approach is not valid for inelastic scattering process (Jacoboni and Lugli, 1989). Because of this the calculation of polar optic phonon scattering is used the other numerical method instead of relaxation time approach. In this work it was used an iterative method for the calculation.

MODEL DETAILS

The present calculations of electron mobility are based on solving Boltzmann transport equation with iterative method (Liu et al., 2000). Rode's iterative technique provides a compact method of solution of the Boltzmann equation in the low field regime (Ridley, 1997). To derive Rode's method, we start with the Boltzmann transport equation for the case of steady-state conditions and no spatial gradients.

$$\frac{\partial f}{\partial t} + v.\nabla_r f + \frac{eF}{\hbar}.\nabla_k f = \left(\frac{\partial f}{\partial t}\right)_{coll} \tag{1}$$

Where $(\partial f/\partial t)_{coll}$ represents the change of distribution function due to the electron scattering. In the steady-state and under application of a uniform electric field the Boltzmann equation can be written as

$$\frac{eF}{\hbar}.\nabla_k f = \left(\frac{\partial f}{\partial t}\right)_{coll} \tag{2}$$

Consider electrons in an isotropic, non-parabolic conduction band whose equilibrium Fermi distribution function is $f_0(k)$ in the absence of electric field. Note the equilibrium distribution $f_0(k)$ is isotropic in k space but is perturbed when an electric field is applied. If the electric field is small, we can treat the change from the equilibrium distribution function as a perturbation which is first order in the electric field. The distribution in the presence of a sufficiently small field can be written quite generally as

$$f(k) = f_0(k) + f_1(k)\cos\theta \tag{3}$$

Where θ is the angle between k and F and $f_1(k)$ is an isotropic function of k, which is proportional to the magnitude of the electric field. f(k) satisfies the Boltzmann Equation 2 and it follows that

$$\frac{eF}{\hbar}\frac{\partial f_0}{\partial t} = \sum_i \int \left\{ \cos\varphi f_1'[s_i'(1-f_0)+s_i f_0]d^3k' - f_1 \int [s_i(1-f_0')+s_i'f_0']d^3k' \right\} \tag{4}$$

In general there will be both elastic and inelastic scattering processes. For example impurity scattering is elastic and acoustic and piezoelectric scattering are elastic to a good approximation at room temperature. However, polar and non-polar optical phonon scattering are inelastic. Labeling the elastic and inelastic scattering rates with subscripts el and inel respectively and recognizing that, for any process i, $s_{eli}(k', k) = s_{eli}(k, k')$ equation 4 can be written as

$$f_1(k) = \frac{\frac{-eF}{\hbar}\frac{\partial f_0}{\partial k} + \sum \int f_1'\cos\varphi[s_{inel}'(1-f_0)+s_{inel}f_0]d^3k'}{\sum \int (1-\cos\varphi)s_{el}d^3k' + \sum \int [s_{inel}(1-f_0')+s_{inel}'f_0']d^3k'} \tag{5}$$

Note the first term in the denominator is simply the momentum relaxation rate for elastic scattering. Equation 5 may be solved iteratively by the relation

$$f_{1n}(k) = \frac{\frac{-eF}{\hbar}\frac{\partial f_0}{\partial k} + \sum \int f_1(k')[n-1]\cos\varphi[s_{inel}'(1-f_0)+s_{inel}f_0]d^3k'}{\sum \int (1-\cos\varphi)s_{el}d^3k' + \sum \int [s_{inel}(1-f_0')+s_{inel}'f_0']d^3k'} \tag{6}$$

Where $f_{1n}(k)$ is the perturbation to the distribution function after the n-th iteration. It is interesting to note that if the initial distribution is chosen to be the equilibrium distribution, for which $f_1(k)$ is equal to zero, we get the relaxation time approximation result after the first iteration. We have found that convergence can normally be achieved after only a few iterations for small electric fields. Once $f_1(k)$ has been evaluated to the required accuracy, it is possible to calculate quantities such as the drift mobility μ, which is given in terms of spherical coordinates by

$$\mu = \frac{\hbar}{3m^*F}\frac{\int_0^\infty (k^3/1+2\alpha F)f_1 d^3k}{\int_0^\infty k^2 f_0 d^3k} \tag{7}$$

Here, we have calculated low field drift mobility in ZnS and ZnSe crystal structures using the iterative technique. The effects of piezoelectric, acoustic deformation, polar optical phonons and ionized impurity scattering have been included in the model. It is also assumed that the electrons remain in the Γ-valley of the Brillouin zone. Further we supposed that the materials have the isotropic nonparabolic band structure. We took into account electron screening and mixing of s and p wave functions.

LOW-FIELD TRANSPORT RESULTS IN ZnS AND ZnSe

In the work, electron mobility for ZnS and ZnSe compounds are calculated using iterative method. We investigated temperature and doping dependencies of electron mobility in range of 150 to 500 K. The electron concentration of ZnS and ZnSe compounds was taken as 10^{22}, 10^{23} and 10^{24} m^{-3}. Further in this work we calculated the mobility for various concentrations. Important parameters used throughout the calculations are listed in Table 1.

Figure 1 shows the calculated electron drift mobilities versus temperature and donor concentration for ZnS and ZnSe compounds. The electron drift mobilities at room temperature that we find are 1250 and 1050 cm^{2}V^{-1}s^{-1} for ZnSe and ZnS structures, respectively, for an electric field equal to 10^4 Vm^{-1} and with a donor concentration of 10^{23} m^{-3}. The material parameters used to calculate the electron drift mobilities are tabulated in Table 1.

The results plotted in figure 1a indicate that the electron drift mobility of ZnS is lower than that for the ZnSe structure. This is largely due to the higher ℘ valley

Table 1. Important parameters used in our calculations for ZnS and ZnSe materials which are taken from references (Chattopadhyay and Queisser, 1981).

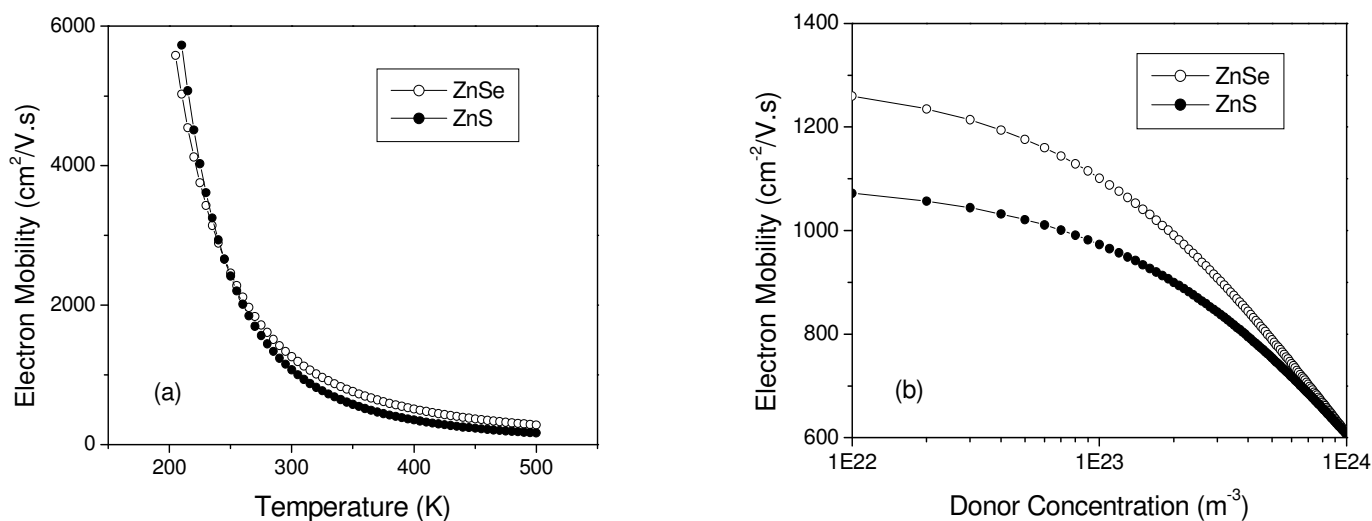|	ZnS	ZnSe
Density ρ (kgm^{-3})	4075	5420
Longitudinal sound velocity v_s (ms^{-1})	5668	4580
Low-frequency dielectric constant ε_s	9.6	9.2
High-frequency dielectric constant ε_∞	5.7	15
Acoustic deformation potential (eV)	4.9	4.5
Polar optical phonon energy (eV)	0.0426	0.0314
Γ-valley effective mass (m*)	0.28	0.17
Γ-valley non-parabolicity (eV^{-1})	0.69	0.67

Figure 1. (a) Electron drift mobility of ZnS and ZnSe structures versus temperature. Donor concentration is approximately 10^{23} m^{-3}, (b) Electron drift mobility of ZnS and ZnSe structures versus donor concentration at room temperature.

effective mass in the ZnS structure.

Figure 1b shows the calculated variation of the electron mobility as a function of the donor concentration for both ZnS and ZnSe crystal structures at room temperature.

The mobility does not vary monotonically between donor concentrations of 10^{22} m^{-3} and 10^{24} m^{-3} due to the dependence of electron scattering on donor concentration, but shows a maximum at 10^{22} m^{-3} for both compounds.

In order to understand the scattering mechanisms which limit the mobility of ZnS and ZnSe under various conditions, we have performed calculations of the electron drift mobility when particular scattering processes are ignored. The solid circle curve in Figure 2 shows the calculated mobility for ZnS material including all scattering mechanisms whereas the open circle and star curves show the calculated mobility without ionized impurity and polar optical scattering, respectively. It can be seen that below 250 K the ionized impurity scattering is dominant while at the higher temperatures electron

scattering is predominantly by optical modes. Thus the marked reduction in mobility at low temperatures in Figure 2 can be ascribed to impurity scattering and that at high temperatures to polar optical phonon scattering.

The temperature variation of the electron drift mobility in ZnS and ZnSe compounds for different donor concentrations is shown in Figure 3. It is evident from this figure that the curves approach each other at very high temperatures, where the mobility is limited by longitudinal optical phonon scattering, whereas the mobility varies inversely with donor concentration at low temperatures as we would expect from the foregoing discussion.

Conclusions

In conclusion, we have studied the electron transport characteristic associated with ZnS and ZnSe compounds. Temperature dependent and free electron concentration dependent of the electron mobility in both structures have
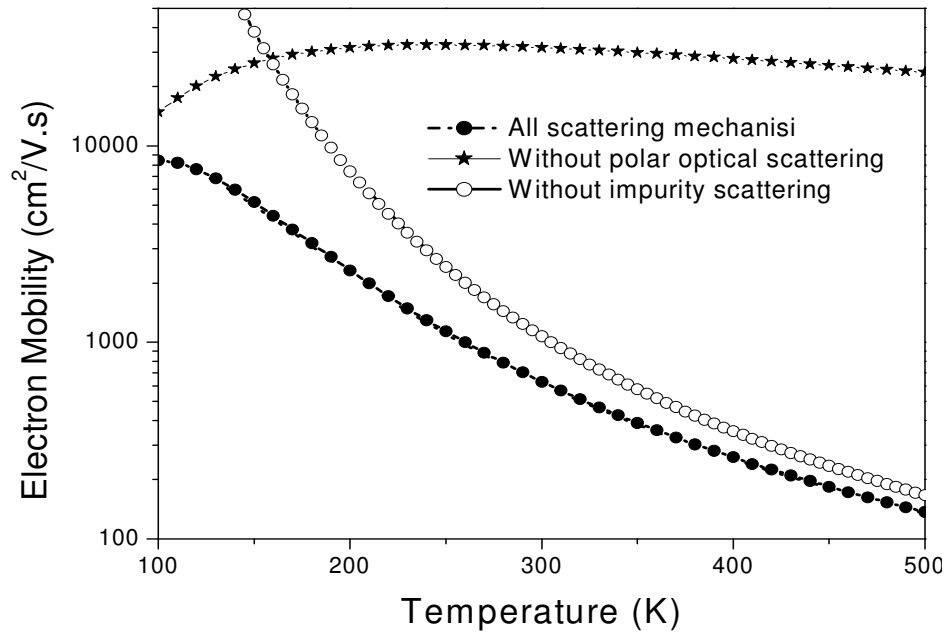
Figure 2. Comparison of electron drift mobility ZnS material with donor concentration of 10^{23} m^{-3} and when individual scattering processes are ignored.
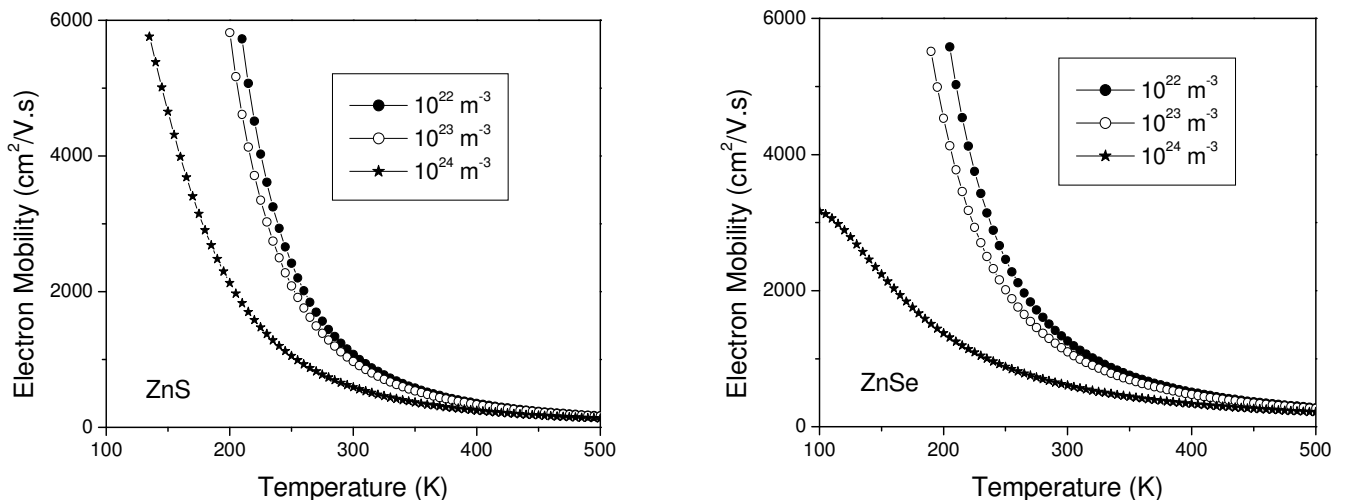

Figure 3. Calculated low-field electron drift mobility of ZnS and ZnSe compounds as functions of temperature for different donor concentrations.

been compared. It has been found that the low-field electron mobility is significantly higher for the ZnSe structure than ZnS structure due to the lower Γ electron effective mass in this crystal structure. Several scattering mechanisms have been included in the calculation. Ionized impurities have been treated beyond the born approximation using a phase shift analysis. Screening of ionized impurities has been treated more realistically using a multi-ion screening formalism, which is more relevant in the case of highly compensated III-V semiconductors.

REFERENCES

Brennan K (1998). Monte Carlo study of electron transport in ZnS, J. Appl. Phys., 64: 4024.

Chattopadhyay D, Queisser HJ (1981). Monte Carlo simulation in ZnS devices. Rev. Modern Physics, p. 53.

Chen Y, Bagnall DM, Koh HJ, Park KT, Zhu ZQ, Yao T (1998). Hall Mobility in GaN material. J. Appl. Phys., 84: 3912.

Di K, Brennan K (1991). Comparison of electron transport properties in ZnS and ZnSe. J. Appl. Phys., 69: 3097.

Jacoboni C, Lugli P (1989). Zhe Monte Carlo Method for semiconductor and Device Simulation, Springer-Verlag.

Liu Y, Gorla CR, Liang S, Emanetoglu N, Wraback M (2000). Crystal growth in ZnS. J. Electron Mater., 29: 69.

Look DC, Reynolds DC, Sizelove JR, Harsch WC (1998). Effect of plasmon scattering in semiconductor devices. Solid Stat. Commun., 105: 399.

Makino T, Segawa Y, Ohtomo A (2001). Electron mobility in high electric field application. Appl. Phys. Lett., 78: 1237.

Mansour N, Di K, Brennan K (2000). Full band Monte Carlo simulation in GaN material. J. Appl. Phys., 70: 6854.

Moglestue C (1993). Monte Carlo Simulation of Semiconductor Devices, Chapman and Hall.

Ridley BK (1997). Electrons and phonons in semiconductor multilayers, Cambridge University Press.